sustainability

MDPI

Article

Firefly Optimization Heuristics for Sustainable Estimation in Power System Harmonics

Naveed Ahmed Malik [1], Naveed Ishtiaq Chaudhary [2] and Muhammad Asif Zahoor Raja [2,*]

[1] Graduate School of Engineering Science and Technology, National Yunlin University of Science and Technology, 123 University Road, Section 3, Douliou, Yunlin 64002, Taiwan
[2] Future Technology Research Center, National Yunlin University of Science and Technology, 123 University Road, Section 3, Douliou, Yunlin 64002, Taiwan
* Correspondence: rajamaz@yuntech.edu.tw

Abstract: The sustainable power development requires the study of power quality while taking into account of electrical equipment is an important aspect because it highly compromises the overall efficiency including quality, reliability and continuity of power flow. The aim for smooth power flow is only accomplished if compatibility is met between all the instruments connected to the system. The odd harmonics both on amplitude and phase domain must be known in order to exactly cop up with their adverse effects on overall working of the system. In this regard, parameter estimation is performed in detail for diverse generation size (gs) and particle size (ps), besides for altered signal to noise ratio. Firefly optimization technique under different scenarios for both phase and amplitude parameters accurately estimated the power signal harmonics and proved its robustness under different noise levels. The MSE values achieved by FFO are 6.54×10^{-3}, 1.04×10^{-5} and 1.35×10^{-6} for 20 dB, 50 dB and 80 dB respectively for gs = 200 in case study 1. While the respective results in case study 2 are 7.33×10^{-3}, 6.67×10^{-6} and 6.59×10^{-9} for gs = 1000. Whereas no significant effect in performance is seen with the change in ps values.

Keywords: parameter estimation; harmonics; firefly optimization; swarm intelligence

check for updates

Citation: Malik, N.A.; Chaudhary, N.I.; Raja, M.A.Z. Firefly Optimization Heuristics for Sustainable Estimation in Power System Harmonics. *Sustainability* **2023**, *15*, 4816. https://doi.org/10.3390/su15064816

Academic Editor: Gaetano Zizzo

Received: 26 January 2023
Revised: 23 February 2023
Accepted: 6 March 2023
Published: 8 March 2023

Copyright: © 2023 by the authors. Licensee MDPI, Basel, Switzerland. This article is an open access article distributed under the terms and conditions of the Creative Commons Attribution (CC BY) license (https://creativecommons.org/licenses/by/4.0/).

1. Introduction

By the arise of current era, power electronics equipment's have become the most important constituent of electrical systems including variable resistance speed drives, smart computers, auto function protection devices and so on. The proper functionality of these devices mostly depends on the smooth voltage and current waveform which is only achieved by attenuating the harmonics involved in the input voltage and current waveforms [1,2]. Research has been carried out using different methods to analyze the periodic signal contaminated by harmonics and sub harmonics. Numerous techniques for study gathered the attention of harmonics distortion [3–6].

The research community proposed various schemes for powers signals estimation [7–9] and a number of papers have been presented in the literature that pivots the estimation of harmonics contamination [10]. These techniques include fast harmonics estimation using EA-AWNN by Sachin K. Jain et al. [11], exponential modulation integral observer by Hin Say Lam et al. [12], compressive sensing by Palczynska [13], Bayesian approach used by Gabriele D Antona et al. [14], ESPIRIT associated filter bank scheme by Santos [15], Kalman filter [16,17], least mean square based algorithms [18,19], and recursive least square strategy [20].

The concept of population search based optimization through swarm/evolutionary heuristics has been emerged over the recent years with excellent performance in solving various engineering and applied sciences problems [21–25]. The metaheuristics are also exploited for optimization of power systems [26–30], as well as harmonics estimation, such as, neuro evolutionary approach [31], evolutionary technique [32], grey wolf optimizer [33],

particle swarm optimizer (PSO) [34–36], artificial bee colony [37–39], biogeography based optimization [40], fractional order PSO [41] and cuckoo search optimization [42].

The swarm intelligence based firefly optimization (FFO) algorithm has shown excellent performance in solving nonlinear and multimodal problems [43–45]. The FFO has been effectively applied to solve point tracking of PV systems [46–48], job scheduling [49], fraud detection [50], material sciences [51], energy management [52], flying adhoc networks [53], automatic data clustering [54,55], resonant accelerometers [56], multi robot foraging [57], load balancing [58] and many others. The brilliant performance of the FFO for these spectrum of challenging problems motivates the authors to exploit the optimization strength of the FFO for power systems harmonics estimation. In this paper the domain of work is further extended using a nature inspired heuristic technique based on FFO algorithm that focuses on the estimation of harmonics pollution. The main contributions/salient features of the proposed study are:

- The swarm intelligence of firefly optimization approach is exploited for sustainable power development through effective harmonics estimation arising in industrial loads.
- The phase and amplitude variables related to the first, third, fifth and eleventh harmonics are effectively estimated using optimization knacks of firefly algorithm.
- The FFO shows stupendous performance in both examples of harmonics estimation with enhanced accuracy for increased particle size.
- The proposed scheme of FFO is robust, convergent and stable for different signal to noise scenarios in case varying particle and generation size.

The rest of the article is organized as: the harmonics estimation scheme is presented in Section 2, firefly based swarm intelligence approach is given in Section 3, the experimental simulation results are provided in Section 4, and concluding remarks of the investigation are presented in Section 5.

2. Materials and Methods

The multi frequency sinusoidal signal in terms of amplitude λ, angular frequency ω and phase μ is defined as:

$$g(t) = \lambda_1 \sin(\omega_1 t + \mu_1) + \lambda_2 \sin(\omega_2 t + \mu_2) + \cdots + \lambda_M \sin(\omega_M t + \mu_M). \quad (1)$$

Considering the noise $\varepsilon(t)$ in the (1) and writing in compact form

$$g(t) = \sum_{m=1}^{M} \lambda_m \sin(\omega_m t + \mu_m) + \varepsilon(t). \quad (2)$$

The signal presented in Equation (2) is sampled with h period, $t_k = kh$ and $g(t_k) = g(k)$ provides

$$g(k) = \sum_{m=1}^{M} \lambda_m \sin(\omega_m k + \mu_m) + \varepsilon(k). \quad (3)$$

Applying the trigonometric identity, sin (α + β) = sinαcosβ + cosαsinβ to (3) yields

$$g(k) = \sum_{m=1}^{M} [\lambda_m \{\sin(\omega_m k) \cos \mu_m + \cos(\omega_m k) \sin \mu_m\}] + \varepsilon(k). \quad (4)$$

Supposing

$$x_m = \lambda_m \cos \mu_m \text{ and } y_m = \lambda_m \sin \mu_m, \quad (5)$$

Using (5) in (4)

$$g(k) = \sum_{m=1}^{M} [x_m \sin(\omega_m k) + y_m \cos(\omega_m k)] + \varepsilon(k). \quad (6)$$

Defining the intermediate parameter vector $\mathbf{\Theta}$ in (7), the corresponding information vector $\mathbf{\Omega}$ in (8) and the identification model in (9)

$$\mathbf{\Theta} = [x_1, y_1, x_2, y_2, \ldots, x_m, y_m], \tag{7}$$

$$\mathbf{\Omega}(k) = [\sin(\omega_1 k), \cos(\omega_1 k), \sin(\omega_2 k), \cos(\omega_2 k), \ldots, \sin(\omega_m k), \cos(\omega_m k)] \tag{8}$$

The actual parameters, i.e., amplitude λ and phase μ are obtained by using the intermediate parameters through the following relations

$$\lambda_m = \sqrt{(x_m)^2 + (y_m)^2}, \mu_m = \tan^{-1} \frac{y_m}{x_m}. \tag{9}$$

The criterion function based on the difference between actual $g(k)$ and estimated $g'(k)$ signal in mean square sense is defined as

$$\Psi(k) = \text{mean}\left[g(k) - g'(k)\right]^2 = \left[g(k) - \mathbf{\Omega}^T(k)\mathbf{\Theta}'\right]^2 \tag{10}$$

3. Optimization Scheme: Firefly Algorithm

In 2008 Yang et al., put forward an algorithm that was inspired on the basis of the flaring attribute of fire flies with clear explaination using following three rules;

(i) Fire flies are unisex, so the probability of attraction on the basis of sex is zero.
(ii) Since brightness is the key characteristic of a firefly. So the brighter firefly will tend to fly towards the less bright firefly. The relationship between the attractiveness and brightness is inverse with respect to the distance, i.e., brightness will decrease if the distance is increased and vice versa. In this manner, relationship maintained randomness between the firefly movements.
(iii) Brightness is associated key factor in construction of the problem specific objective function.

The dissimilarity in light intensity and attractiveness of the fireflies are two important factors of the interest. Attractiveness in the firefly measure on brightness quality, i.e., the attractiveness is defined on the basis of brightness. This brightness B of the fire fly at a specific position x is directly to the maximization of objective function f and is mathematically expressed as follows:

$$B(x) \propto f(x). \tag{11}$$

In this scenario, the attractiveness A is relative to the eyes of the observer or distance d_{ij} between the firefly i^{th} and j^{th}. In mathematical form, brightness B depends upon the distance d, i.e., it exponential function representation is given as:

$$B = B_o e^{-\gamma d}. \tag{12}$$

In the above expression B_o is the original brightness and γ is the coefficient of light absorption. In attractiveness representive with A in terms of the exponential function is given as:

$$A = A_o e^{-rd^2}, \tag{13}$$

where A_o is the attractiveness at d = 0. Replacing exponent rd by rd^m (m > 0). Between two fireflies i and j, the distance between x_j and x_j are the Cartesian distance

$$r_{ij} = ||x_i + x_j||_2. \tag{14}$$

The motion of the firefly i is fascinated by firefly j and is set on by

$$x_i = x_i + A_0 e^{-\gamma r^2{}_{ij}}(x_j - x_i) + \alpha\varepsilon_i. \tag{15}$$

In above expression, ε_i is the vector of randomization and can be pinched by Gaussian distribution and in most cases we take $A^o = 1$, $\alpha \epsilon [0, 1]$ and $\gamma = 1$.

The difference in the attractiveness is characterized by γ and its value is very important to determine the speed of convergence and also FFO behavior. Theoretically, we have $\Gamma \epsilon [0, \infty]$ but in practical/generally we assume $\gamma \epsilon [0, 1]$. If $\gamma = 0$ the attractiveness is considered constant $A = A_o$. This means that the brightness B remains constant and flashing firefly can be visualized in any dominion. If the firefly is moving in a misty area, the attractiveness is almost zero. This corresponds to an exceptional case of PSO. Thus if the nested loop for j^{th}. firefly is eliminated and A^j is put back by the current *g - best*, the potential efficiency of FFO becomes equal to PSO in this special case. Now if $\gamma \longrightarrow \infty$, we have $A(r) \longrightarrow \partial(r)$, which is Dirac ∂ -function and the attractiveness is totally blur, which means it becomes zero again or fireflies become short sighted. No other fireflies are seen in very foggy region and each firefly moves in a random way. For that reason, this leads to the completely random search method. The flow chart of the FFO is provided in Figure 1, while the graphical abstract of the proposed study is given in Figure 2. The electrical circuit given in part 1 of Figure 2 is the general circuit producing the basic signal and then the general representation of the harmonics corrupted signal is provided. While part 2 provides the mathematical representation of the problem and fitness function formulation. The part 3 of the Figure 2 describe the optimization procedure and last part reflects the results obtained from the FFO scheme.

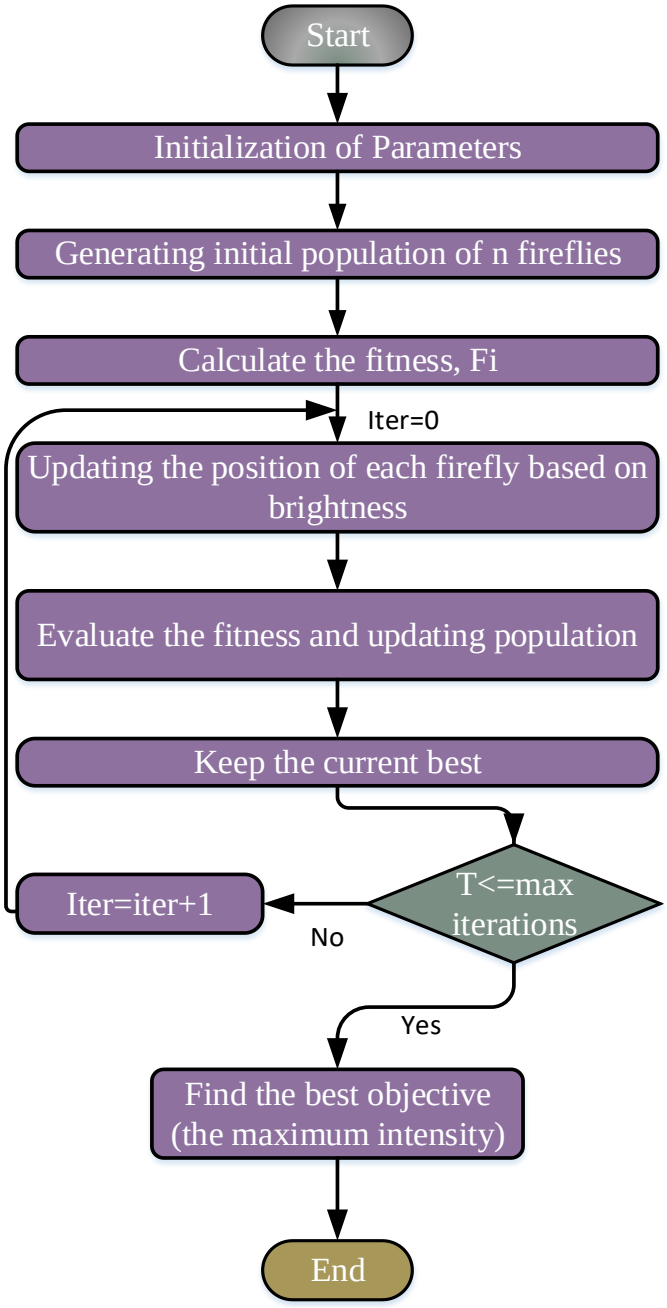

Figure 1. Flow chart of FFO scheme.

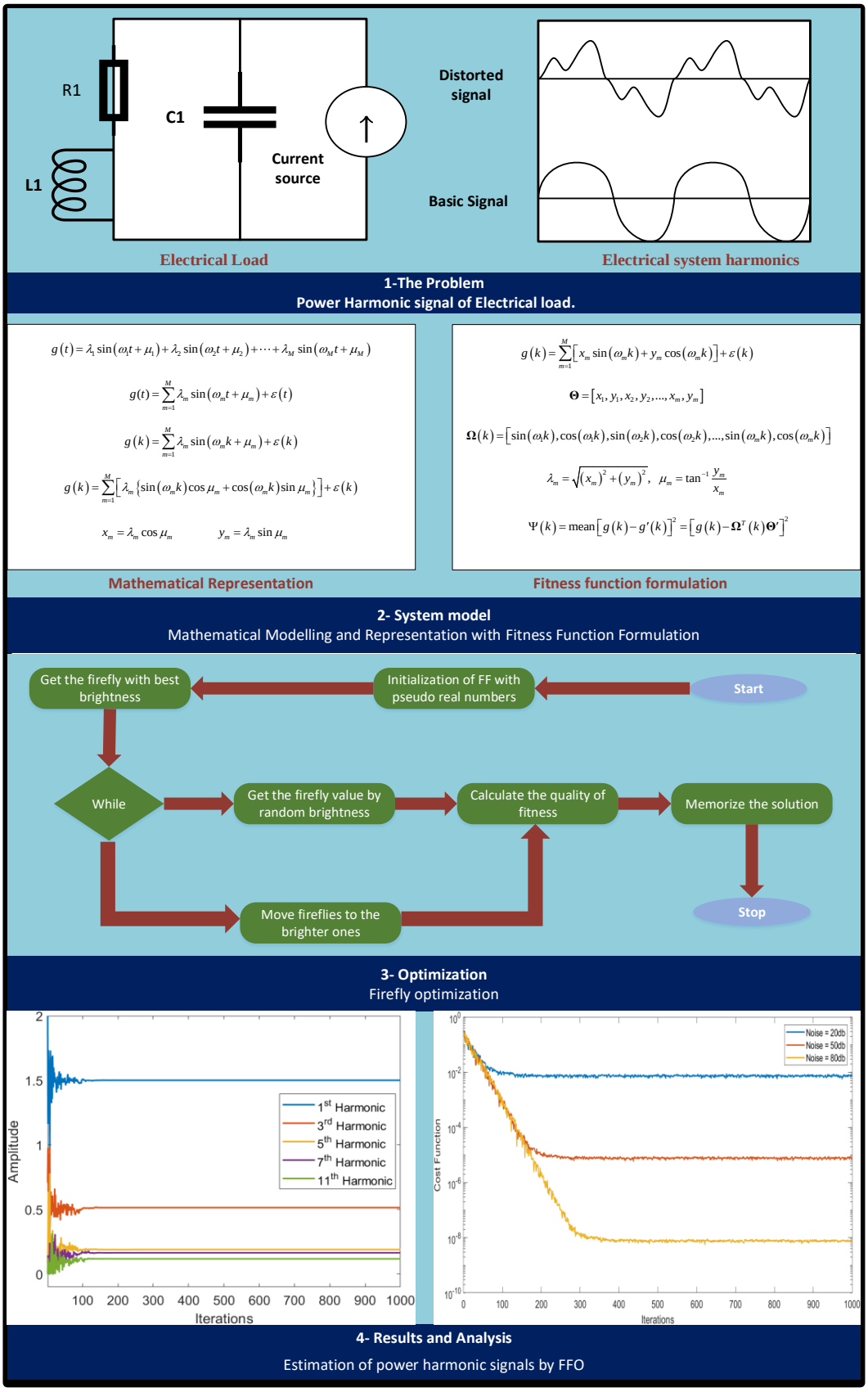

Figure 2. Graphical abstract of the study.

4. Results and Discussion

Fire fly optimization algorithm is applied in this research area for accurate estimation of power signal under two scenarios for different generations and results are stored in tables provided in this section along with graphs. All the simulation work is carried out on Matlab with sampling frequency of 2 kHz. White Gaussian noise is introduced for three levels i.e., ε = 20 dB, 50 dB and 80 dB to evaluate the robustness and accuracy of the system for real time scenarios. For each scenario the investigation is carried out for four generation size (gs) and also three particle sizes (ps) for monitoring the behavior of system under different conditions. The values taken are gs = 100, 200, 300 and 400 for example no 1 with ps = 20, 50 and 100. The parameters of the algorithm are selected analytically with great care based on the experience and understanding of the optimization problem to ensure maximum performance.

Case study 1: The harmonic signal taken in first study is

$$h(t) = \begin{bmatrix} 1.5\sin(2\pi f_1 t + 1.396) + 0.5\sin(2\pi f_3 t + 1.047) + 0.2\sin(2\pi f_5 t + 0.785) \\ +0.15\sin(2\pi f_7 t + 0.628) + 0.1\sin(2\pi f_{11} t + 0.523) \end{bmatrix} \quad (16)$$

The total number of variables taken are ten including five phase and five amplitude parameters as;

$$\begin{aligned} \zeta &= [\lambda_1, \lambda_2, \lambda_3, \lambda_4, \lambda_5, \mu_1, \mu_2, \mu_3, \mu_4, \mu_5] \\ &= [1.50, 0.50, 0.20, 0.15, 0.10, 1.396, 1.047, 0.785, 0.628, 0.523] \end{aligned} \quad (17)$$

Case study 2: The harmonic signal considered in second study is

$$h(t) = \begin{bmatrix} 1.2\sin(2\pi f_1 t + 1.309) + 0.8\sin(2\pi f_3 t + 0.959) + 0.2\sin(2\pi f_5 t + 0.785) \\ +0.18\sin(2\pi f_7 t + 0.698) + 0.1\sin(2\pi f_{11} t + 0.523) \end{bmatrix} \quad (18)$$

The five amplitude and five phase parameters is

$$\begin{aligned} \zeta &= [\lambda_1, \lambda_2, \lambda_3, \lambda_4, \lambda_5, \mu_1, \mu_2, \mu_3, \mu_4, \mu_5] \\ &= [1.20, 0.80, 0.20, 0.18, 0.10, 1.309, 0.959, 0.785, 0.698, 0.523] \end{aligned} \quad (19)$$

The results of case study 1 in terms of parameter estimates through FFO along with the MSE value are given in Tables 1–4 for gs = 100, 200, 300 and 400 respectively. While the respective results in case of Example 2 are presented in Tables 5–8 for gs = 500, 1000, 1500 and 2000. The FFO achieves the MSE values of 6.54×10^{-3}, 1.04×10^{-5} and 1.35×10^{-6} for 20 dB, 50 dB and 80 dB respectively for gs = 200 in case study 1. While the respective results in case study 2 are 7.33E $\times 10^{-3}$, 6.67×10^{-6} and 6.59×10^{-9} for gs = 1000. These results indicate the convergent and robust performance of the FFO scheme for harmonics parameter estimation.

Table 1. Outcomes of the FFO in case of case study 1 for gs = 100.

ε	ps	λ_1	λ_2	λ_3	λ_4	λ_5	μ_1	μ_2	μ_3	μ_4	μ_5	Ψ
20	20	1.1548	0.7979	0.2117	0.1976	0.1361	1.3176	0.9549	0.6284	0.6519	0.2675	1.24×10^{-2}
	50	1.2190	0.7730	0.1823	0.2007	0.0881	1.3418	0.9370	0.9831	0.7175	0.6905	1.07×10^{-2}
	100	1.1697	0.7873	0.2086	0.1428	0.0891	1.2897	0.9727	0.8105	0.6601	1.0891	1.02×10^{-2}
50	20	1.1786	0.7907	0.1833	0.1951	0.0959	1.2982	0.9921	0.6189	0.7859	0.8905	2.26×10^{-3}
	50	1.1833	0.8191	0.1811	0.1766	0.1237	1.2945	0.9622	0.8468	0.6749	0.4560	9.98×10^{-4}
	100	1.1867	0.7947	0.2165	0.1675	0.0980	1.3033	0.9600	0.7815	0.5739	0.4477	5.99×10^{-4}
80	20	1.2156	0.7610	0.1899	0.1772	0.0531	1.3378	0.9549	0.8896	0.7150	1.6492	6.02×10^{-3}
	50	1.1965	0.7865	0.1757	0.2092	0.1092	1.3167	0.9645	0.7428	0.8010	0.5862	1.21×10^{-3}
	100	1.2214	0.8028	0.1937	0.1757	0.1032	1.2901	0.9372	0.7409	0.6959	0.6160	6.89×10^{-4}
		1.2000	0.8000	0.2000	0.1800	0.1000	1.3090	0.9590	0.7850	0.6980	0.5230	0

Table 2. Outcomes of the FFO in case of case study 1 for gs = 200.

ε	ps	λ_1	λ_2	λ_3	λ_4	λ_5	μ_1	μ_2	μ_3	μ_4	μ_5	Ψ
20	20	1.2032	0.7803	0.1926	0.1729	0.1062	1.2966	0.9901	0.8137	0.6196	0.3942	7.34×10^{-3}
	50	1.1799	0.7868	0.2064	0.1793	0.0992	1.2912	0.9598	0.8849	0.7747	0.2160	8.80×10^{-3}
	100	1.1879	0.8048	0.2065	0.1669	0.1016	1.2980	0.9482	0.7472	0.6806	0.4741	6.54×10^{-3}
50	20	1.1987	0.7994	0.1989	0.1793	0.0997	1.3044	0.9581	0.7853	0.6957	0.5059	1.29×10^{-5}
	50	1.1999	0.8009	0.1989	0.1804	0.0981	1.3057	0.9583	0.7866	0.6970	0.5187	1.13×10^{-5}
	100	1.2000	0.7997	0.1994	0.1788	0.0998	1.3056	0.9591	0.7874	0.7005	0.5141	1.04×10^{-5}
80	20	1.2016	0.8009	0.2000	0.1792	0.1007	1.3060	0.9582	0.7783	0.6946	0.5268	3.56×10^{-6}
	50	1.1997	0.7998	0.1996	0.1797	0.1003	1.3061	0.9594	0.7878	0.7007	0.5131	1.08×10^{-6}
	100	1.2004	0.7986	0.2001	0.1801	0.1000	1.3062	0.9587	0.7826	0.6998	0.5192	1.35×10^{-6}
		1.2000	0.8000	0.2000	0.1800	0.1000	1.3090	0.9590	0.7850	0.6980	0.5230	0

Table 3. Outcomes of the FFO in case of case study 1 for gs = 300.

ε	ps	λ_1	λ_2	λ_3	λ_4	λ_5	μ_1	μ_2	μ_3	μ_4	μ_5	Ψ
20	20	1.1996	0.7891	0.1962	0.1824	0.0951	1.3113	0.9201	0.6863	0.6163	0.7443	8.62×10^{-3}
	50	1.2018	0.8010	0.2145	0.1910	0.1041	1.3183	0.9547	0.7064	0.6876	0.4976	8.28×10^{-3}
	100	1.1992	0.7987	0.1847	0.1881	0.1046	1.3081	0.9496	0.8449	0.6778	0.6463	6.84×10^{-3}
50	20	1.1996	0.7999	0.1995	0.1799	0.0997	1.3061	0.9593	0.7874	0.6975	0.5251	7.44×10^{-6}
	50	1.2000	0.8005	0.1994	0.1792	0.1001	1.3060	0.9587	0.7846	0.7013	0.5249	8.17×10^{-6}
	100	1.1995	0.7997	0.2001	0.1799	0.1001	1.3061	0.9596	0.7834	0.6994	0.5300	7.13×10^{-6}
80	20	1.2000	0.8000	0.2000	0.1799	0.1000	1.3060	0.9590	0.7850	0.6977	0.5233	1.68×10^{-8}
	50	1.2000	0.8000	0.2000	0.1800	0.1000	1.3059	0.9590	0.7851	0.6981	0.5229	1.36×10^{-8}
	100	1.2000	0.8001	0.2000	0.1799	0.1000	1.3060	0.9590	0.7851	0.6980	0.5232	1.31×10^{-8}
		1.2000	0.8000	0.2000	0.1800	0.1000	1.3090	0.9590	0.7850	0.6980	0.5230	0

Table 4. Outcomes of the FFO in case of case study 1 for gs = 400.

ε	ps	λ_1	λ_2	λ_3	λ_4	λ_5	μ_1	μ_2	μ_3	μ_4	μ_5	Ψ
20	20	1.2090	0.7946	0.2090	0.1866	0.0887	1.3073	0.9423	0.8180	0.6076	0.9990	7.86×10^{-3}
	50	1.2002	0.8059	0.2040	0.1556	0.1129	1.3144	0.9341	0.7539	0.6662	0.5639	8.32×10^{-3}
	100	1.2129	0.8061	0.1857	0.1926	0.1040	1.3080	0.9661	0.7048	0.6267	0.4264	7.69×10^{-3}
50	20	1.2001	0.7998	0.2004	0.1796	0.0992	1.3065	0.9581	0.7875	0.6984	0.5223	7.61×10^{-6}
	50	1.1997	0.8000	0.2005	0.1802	0.1002	1.3060	0.9584	0.7842	0.6975	0.5155	6.85×10^{-6}
	100	1.1999	0.8004	0.2001	0.1801	0.1003	1.3060	0.9586	0.7860	0.6968	0.5254	5.89×10^{-6}
80	20	1.2000	0.8000	0.2000	0.1800	0.1000	1.3060	0.9590	0.7850	0.6981	0.5231	7.09×10^{-9}
	50	1.2000	0.8000	0.2000	0.1800	0.1000	1.3060	0.9590	0.7850	0.6980	0.5230	6.57×10^{-9}
	100	1.2000	0.8000	0.2000	0.1800	0.1000	1.3060	0.9590	0.7849	0.6980	0.5231	7.87×10^{-9}
		1.2000	0.8000	0.2000	0.1800	0.1000	1.3090	0.9590	0.7850	0.6980	0.5230	0

Table 5. Outcomes of the FFO in case of case study 2 for gs = 500.

ε	ps	λ_1	λ_2	λ_3	λ_4	λ_5	μ_1	μ_2	μ_3	μ_4	μ_5	Ψ
20	20	1.4797	0.4980	0.2219	0.1534	0.0854	1.4040	1.0635	0.7878	0.4316	0.6992	9.73×10^{-3}
	50	1.4924	0.5094	0.1924	0.1296	0.0978	1.3982	1.0474	0.7031	0.5590	0.5366	7.37×10^{-3}
	100	1.4650	0.4977	0.1999	0.1549	0.0968	1.3915	1.0443	0.7970	0.6036	0.5288	7.96×10^{-3}
50	20	1.5003	0.4999	0.2003	0.1501	0.1002	1.3966	1.0470	0.7865	0.6284	0.5202	8.14×10^{-6}
	50	1.5000	0.5004	0.2006	0.1497	0.1001	1.3958	1.0462	0.7859	0.6314	0.5256	7.23×10^{-6}
	100	1.4998	0.4993	0.1997	0.1501	0.1005	1.3958	1.0477	0.7835	0.6300	0.5251	7.33×10^{-6}
80	20	1.5000	0.5000	0.2000	0.1500	0.1000	1.3960	1.0470	0.7850	0.6280	0.5229	7.93×10^{-9}
	50	1.5000	0.5000	0.2000	0.1500	0.1000	1.3960	1.0470	0.7849	0.6279	0.5229	8.00×10^{-9}
	100	1.5000	0.5000	0.2000	0.1500	0.1000	1.3960	1.0470	0.7850	0.6281	0.5232	7.27×10^{-9}
		1.5000	0.5000	0.2000	0.1500	0.1000	1.3960	1.0470	0.7850	0.6280	0.5230	0

Table 6. Outcomes of the FFO in case of case study 2 for gs = 1000.

ε	ps	λ_1	λ_2	λ_3	λ_4	λ_5	μ_1	μ_2	μ_3	μ_4	μ_5	Ψ
20	20	1.5121	0.5080	0.2013	0.1518	0.1017	1.3837	1.0544	0.7881	0.5550	0.4114	7.74×10^{-3}
	50	1.4865	0.5093	0.1888	0.1561	0.1067	1.3986	1.0470	0.7636	0.5171	0.5950	7.18×10^{-3}
	100	1.4870	0.4935	0.2092	0.1558	0.0952	1.3938	1.0710	0.7631	0.6316	0.3378	7.33×10^{-3}
50	20	1.4999	0.4999	0.2002	0.1498	0.0997	1.3958	1.0465	0.7853	0.6402	0.5186	9.35×10^{-6}
	50	1.5000	0.5000	0.1996	0.1497	0.1005	1.3962	1.0457	0.7846	0.6333	0.5209	7.64×10^{-6}
	100	1.5004	0.5000	0.2000	0.1503	0.1001	1.3960	1.0468	0.7865	0.6279	0.5218	6.67×10^{-6}
80	20	1.5000	0.5000	0.2000	0.1500	0.1000	1.3960	1.0470	0.7850	0.6279	0.5232	8.84×10^{-9}
	50	1.5000	0.5000	0.2000	0.1500	0.1000	1.3960	1.0470	0.7850	0.6281	0.5228	7.82×10^{-9}
	100	1.5000	0.5000	0.2000	0.1500	0.1000	1.3960	1.0470	0.7850	0.6279	0.5231	6.59×10^{-9}
		1.5000	0.5000	0.2000	0.1500	0.1000	1.3960	1.0470	0.7850	0.6280	0.5230	0

Table 7. Outcomes of the FFO in case of case study 2 for gs = 1500.

ε	ps	λ_1	λ_2	λ_3	λ_4	λ_5	μ_1	μ_2	μ_3	μ_4	μ_5	Ψ
20	20	1.4952	0.4994	0.1583	0.1452	0.0646	1.3884	1.1014	0.8158	0.4447	1.3259	1.13×10^{-2}
	50	1.5074	0.4941	0.1758	0.1622	0.0920	1.3972	1.0556	0.8331	0.6290	0.6939	7.44×10^{-3}
	100	1.4872	0.5005	0.2167	0.1631	0.1039	1.3942	1.0575	0.8208	0.6091	0.3720	6.45×10^{-3}
50	20	1.5000	0.5007	0.1998	0.1507	0.1001	1.3959	1.0477	0.7800	0.6237	0.5194	8.55×10^{-6}
	50	1.5005	0.5002	0.2001	0.1500	0.1006	1.3961	1.0468	0.7842	0.6258	0.5296	8.26×10^{-6}
	100	1.4998	0.4999	0.1999	0.1498	0.1000	1.3961	1.0480	0.7828	0.6286	0.5245	7.36×10^{-6}
80	20	1.5000	0.5000	0.2000	0.1500	0.1000	1.3960	1.0470	0.7850	0.6282	0.5230	7.85×10^{-9}
	50	1.5000	0.5000	0.2000	0.1500	0.1000	1.3960	1.0470	0.7849	0.6281	0.5231	7.67×10^{-9}
	100	1.5000	0.5000	0.2000	0.1500	0.1000	1.3960	1.0470	0.7850	0.6281	0.5231	7.59×10^{-9}
		1.5000	0.5000	0.2000	0.1500	0.1000	1.3960	1.0470	0.7850	0.6280	0.5230	0

Table 8. Outcomes of the FFO in case of case study 2 for gs = 2000.

ε	ps	λ_1	λ_2	λ_3	λ_4	λ_5	μ_1	μ_2	μ_3	μ_4	μ_5	Ψ
20	20	1.5137	0.5157	0.2028	0.1598	0.0820	1.4024	1.0210	0.5951	0.6559	1.1507	1.00×10^{-2}
	50	1.5007	0.5144	0.1893	0.1648	0.1178	1.3930	1.0380	0.7978	0.6760	0.3082	7.38×10^{-3}
	100	1.4934	0.4925	0.1921	0.1622	0.0968	1.3956	1.0293	0.8280	0.7062	0.7294	7.37×10^{-3}
50	20	1.5011	0.4997	0.2001	0.1512	0.0994	1.3959	1.0466	0.7878	0.6249	0.5296	8.12×10^{-6}
	50	1.5000	0.5003	0.1995	0.1499	0.1000	1.3960	1.0452	0.7824	0.6235	0.5258	8.19×10^{-6}
	100	1.4998	0.5000	0.2000	0.1506	0.1000	1.3962	1.0479	0.7853	0.6287	0.5294	7.47×10^{-6}
80	20	1.5000	0.5000	0.2000	0.1500	0.1000	1.3960	1.0470	0.7850	0.6280	0.5234	7.03×10^{-9}
	50	1.5000	0.5000	0.2000	0.1500	0.1000	1.3960	1.0470	0.7850	0.6280	0.5232	6.98×10^{-9}
	100	1.5000	0.5000	0.2000	0.1500	0.1000	1.3960	1.0470	0.7850	0.6280	0.5231	7.67×10^{-9}
		1.5000	0.5000	0.2000	0.1500	0.1000	1.3960	1.0470	0.7850	0.6280	0.5230	0

The learning curves along with convergence plots under different noise levels for case study 1 are given in Figures 3–6 for gs = 100, 200, 300 and 400 respectively while for case study 2, the learning curves and convergence plots are provided in Figures 7–10 for gs = 500, 1000, 1500 and 2000 respectively. The Figures 3–10 consist of seven subfigures (a–g). The learning curves corresponding to the first, third, fifth, seventh and eleventh harmonic amplitude are given in the subfigures (a–c) for noise 20 dB, 50 dB and 80 dB respectively. While, the respective learning curves corresponding to the first, third, fifth, seventh and eleventh harmonic phase are given in the subfigures (d–f). The overall convergence plots based on the fitness function (11) are provided in the subfigures (g). Looking at the tables and plots it is quite obvious that FFO gives better accuracy if we decrease the signal to noise ratio up to 80 dB. Also from the data tabulated in the Tables, it is clear that while increasing the generation size more fitness is achieved.

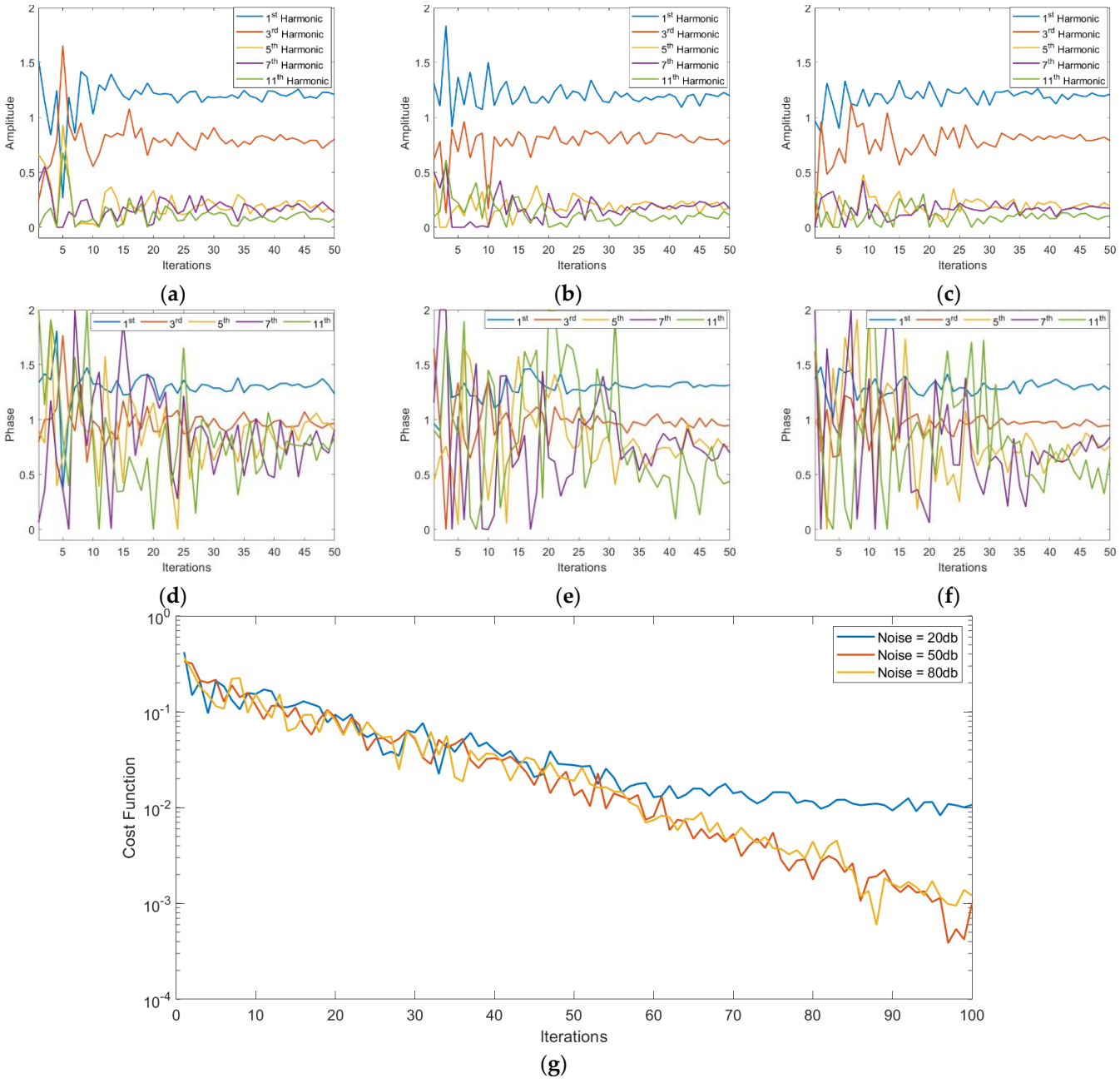

Figure 3. Convergence curves of the harmonic signal in case study 1 for gs = 100. (**a**) amplitude curves for ε = 20 dB; (**b**) amplitude curves for ε = 50 dB; (**c**) amplitude curves for ε = 80 dB; (**d**) phase curves for ε = 20 dB; (**e**) phase curves for ε = 50 dB; (**f**) phase curves for ε = 80 dB; (**g**) learning curves of the cost function.

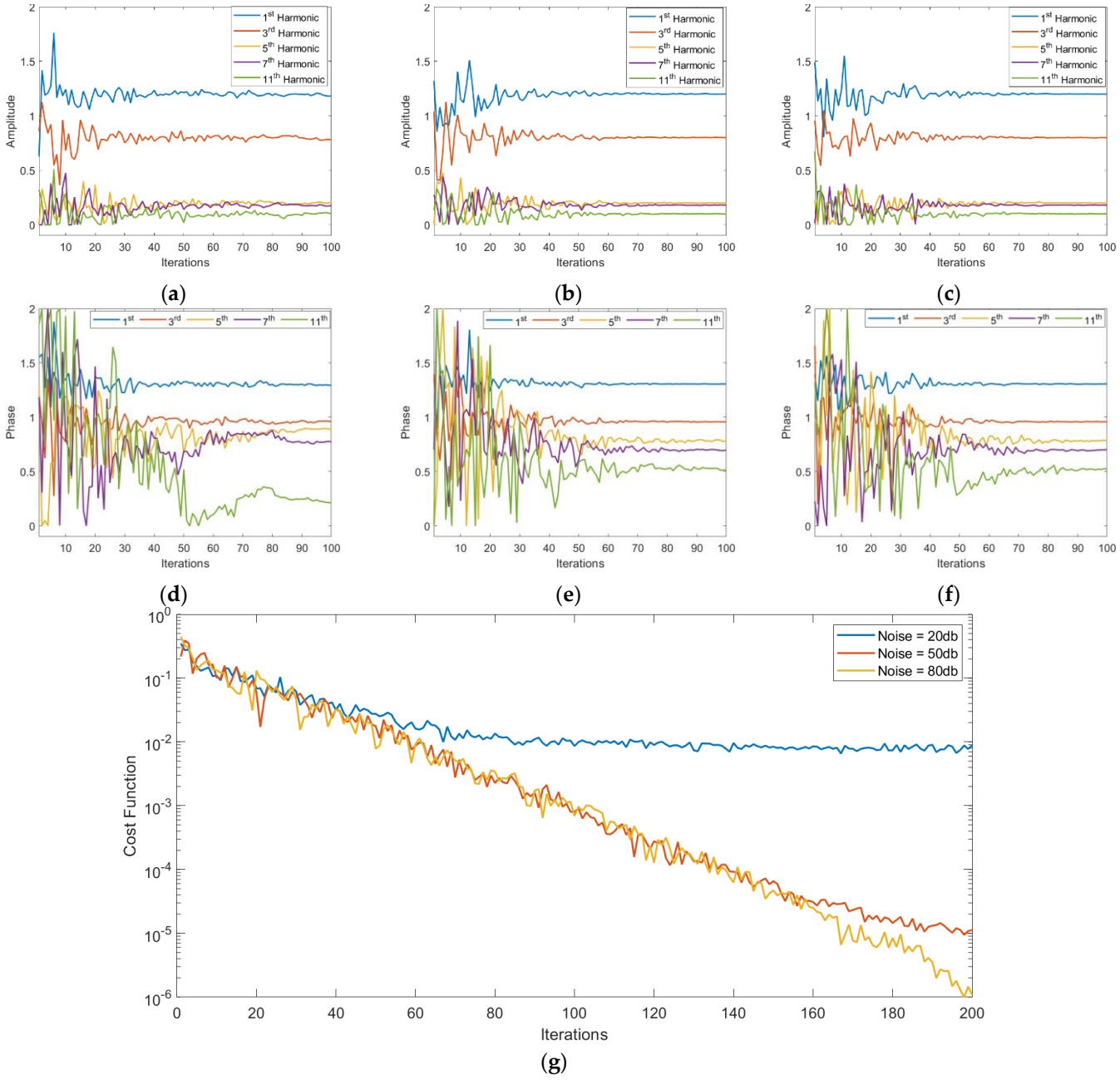

Figure 4. Convergence curves of the harmonic signal in case study 1 for gs = 200. (**a**) amplitude curves for ε = 20 dB; (**b**) amplitude curves for ε = 50 dB; (**c**) amplitude curves for ε = 80 dB; (**d**) phase curves for ε = 20 dB; (**e**) phase curves for ε = 50 dB; (**f**) phase curves for ε = 80 dB; (**g**) learning curves of the cost function.

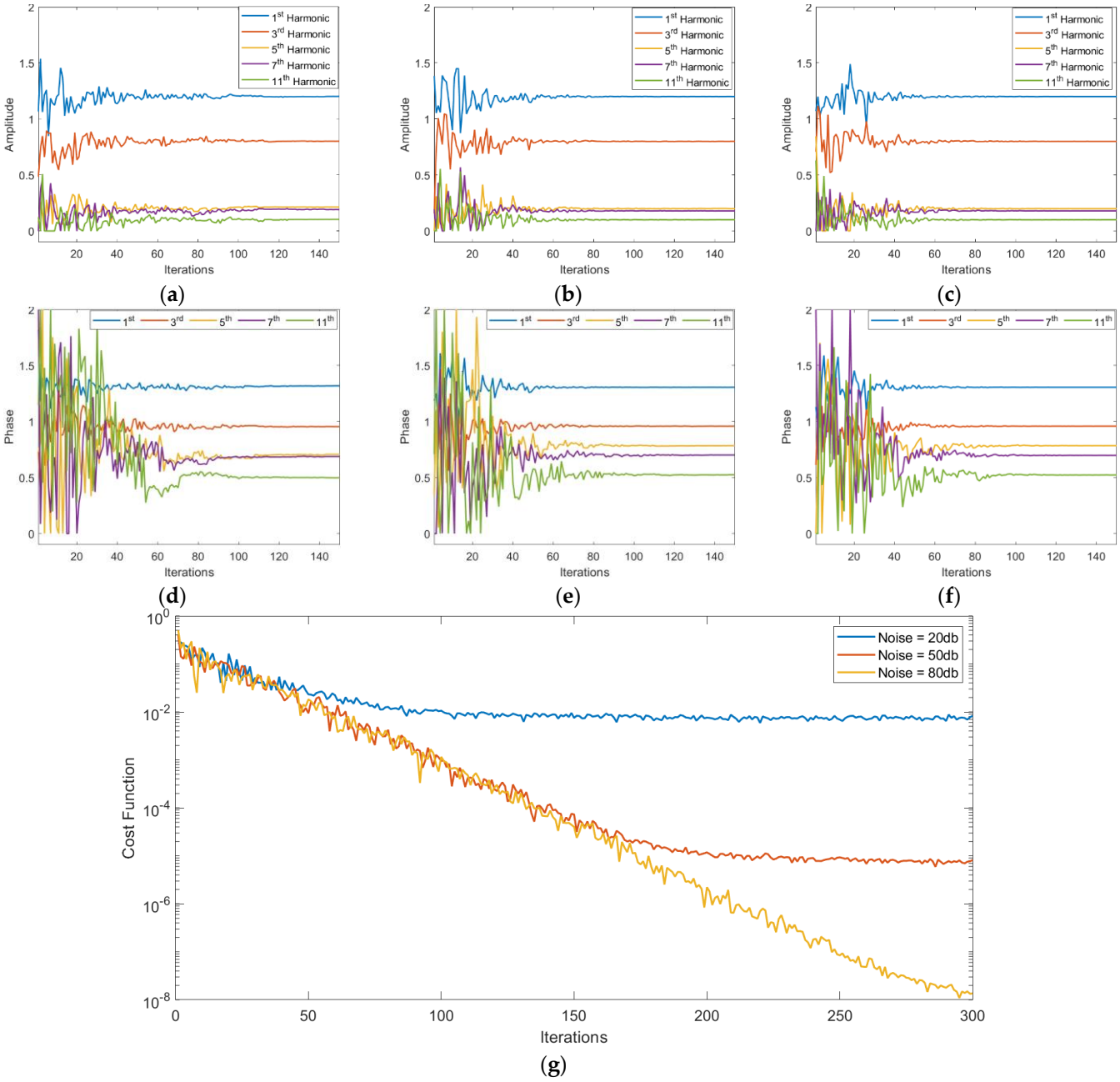

Figure 5. Convergence curves of the harmonic signal in case study 1 for gs = 300. (**a**) amplitude curves for ε = 20 dB; (**b**) amplitude curves for ε = 50 dB; (**c**) amplitude curves for ε = 80 dB; (**d**) phase curves for ε = 20 dB; (**e**) phase curves for ε = 50 dB; (**f**) phase curves for ε = 80 dB; (**g**) learning curves of the cost function.

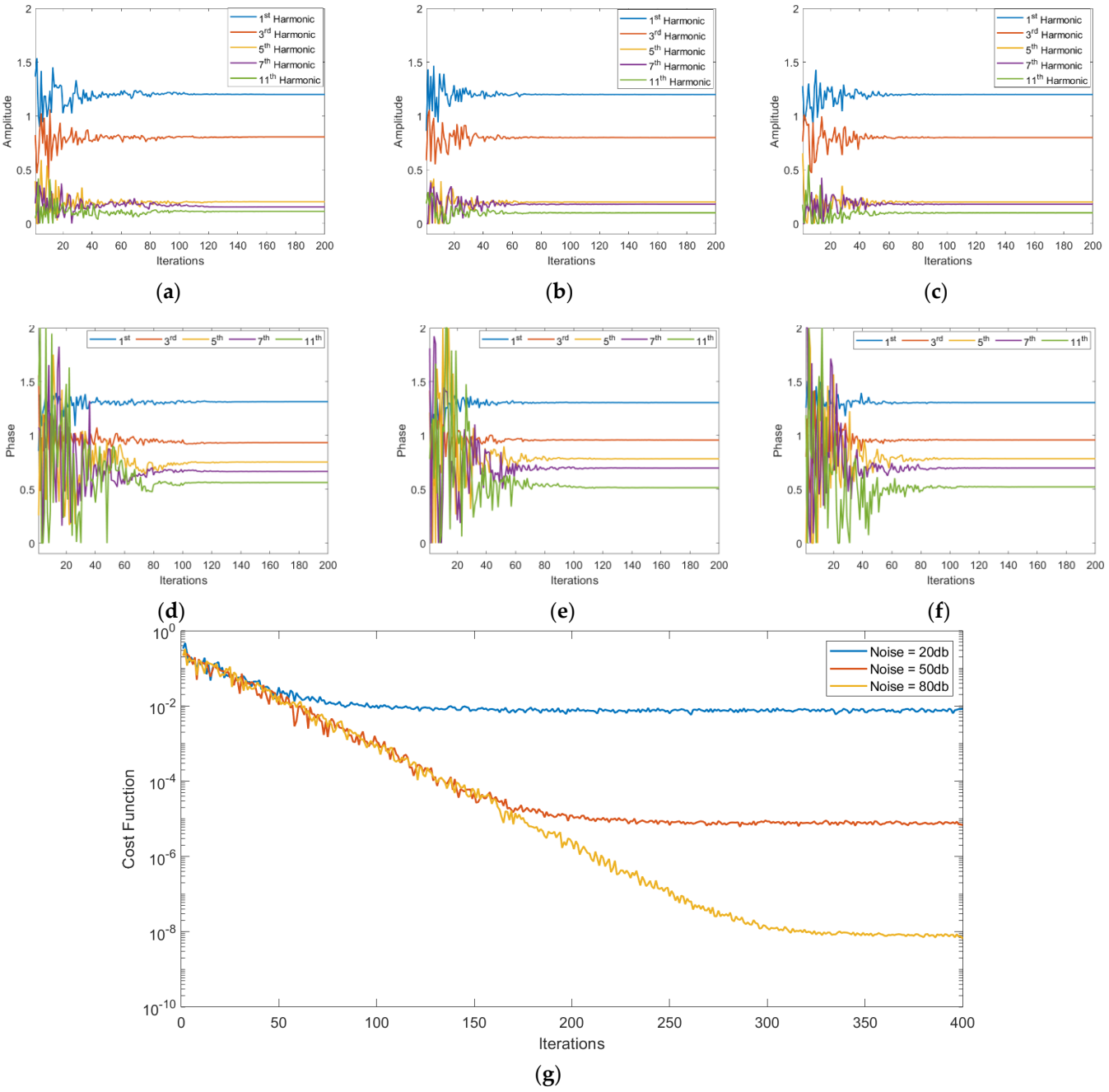

Figure 6. Convergence curves of the harmonic signal in case study 2 for gs = 400. (**a**) amplitude curves for ε = 20 dB; (**b**) amplitude curves for ε = 50 dB; (**c**) amplitude curves for ε = 80 dB; (**d**) phase curves for ε = 20 dB; (**e**) phase curves for ε = 50 dB; (**f**) phase curves for ε = 80 dB; (**g**) learning curves of the cost function.

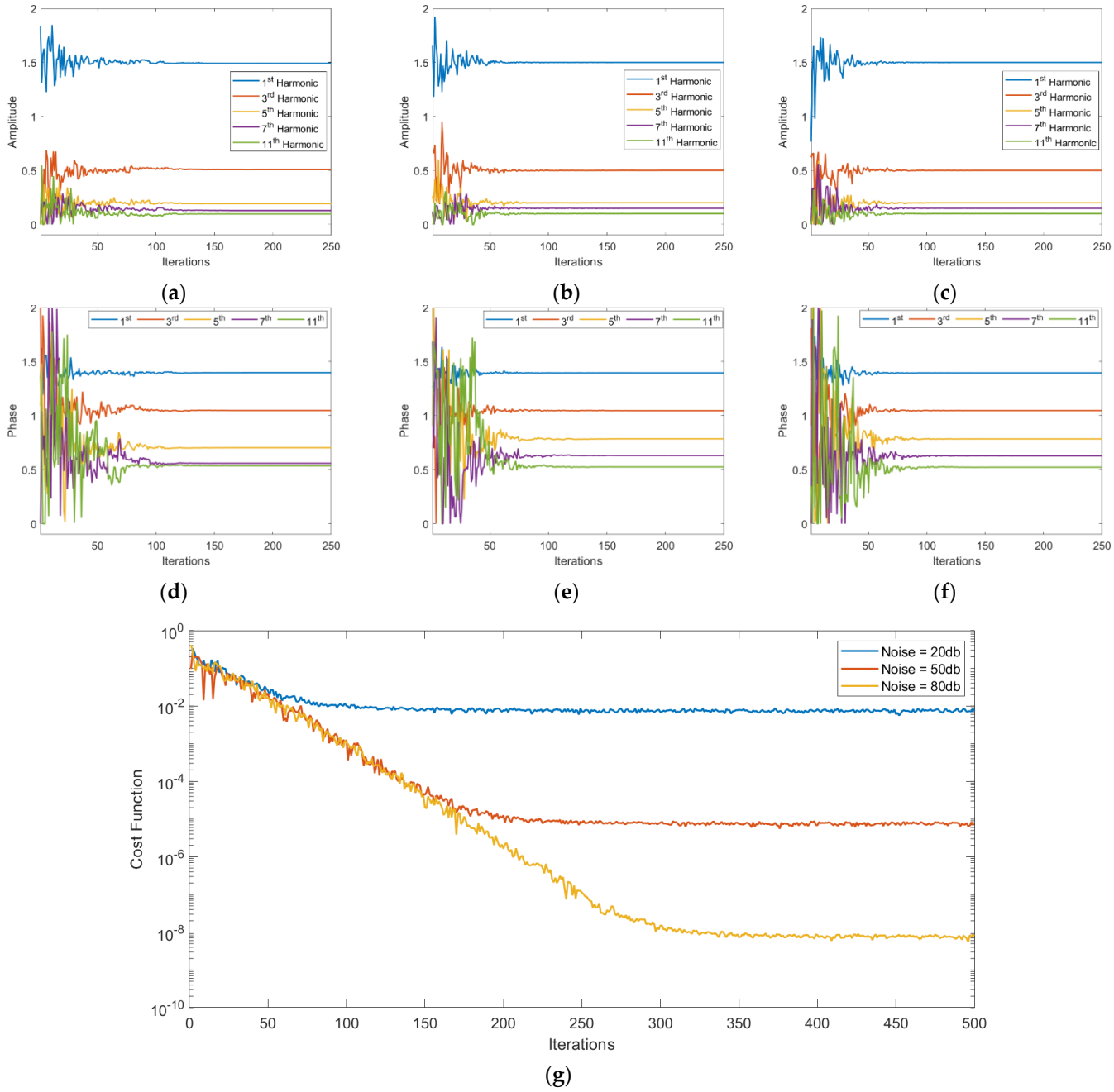

Figure 7. Convergence curves of the harmonic signal in case study 2 for gs = 500. (**a**) amplitude curves for ε = 20 dB; (**b**) amplitude curves for ε = 50 dB; (**c**) amplitude curves for ε = 80 dB; (**d**) phase curves for ε = 20 dB; (**e**) phase curves for ε = 50 dB; (**f**) phase curves for ε = 80 dB; (**g**) learning curves of the cost function.

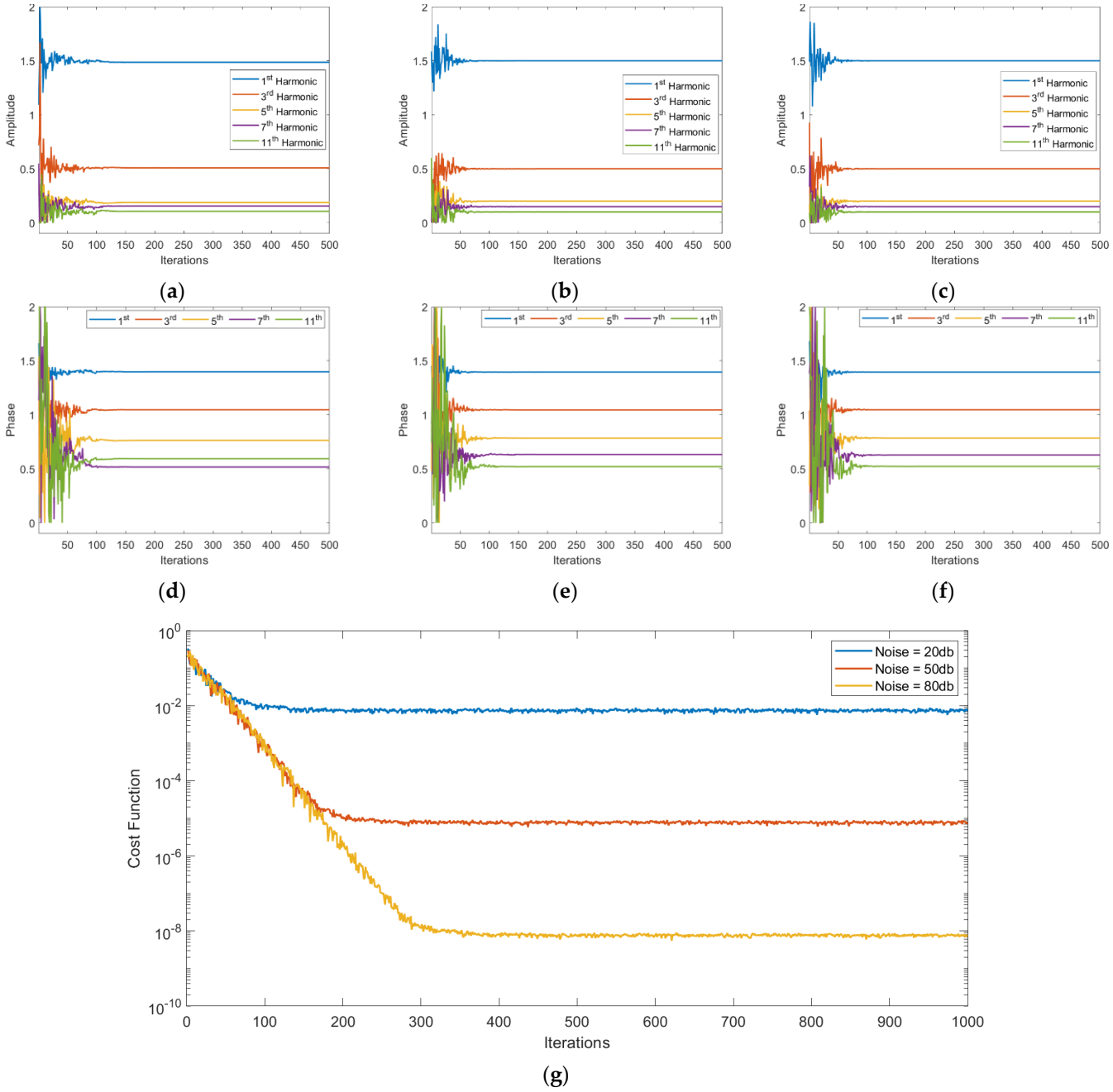

Figure 8. Convergence curves of the harmonic signal in case study 2 for gs = 1000. (**a**) amplitude curves for ε = 20 dB; (**b**) amplitude curves for ε = 50 dB; (**c**) amplitude curves for ε = 80 dB; (**d**) phase curves for ε = 20 dB; (**e**) phase curves for ε = 50 dB; (**f**) phase curves for ε = 80 dB; (**g**) learning curves of the cost function.

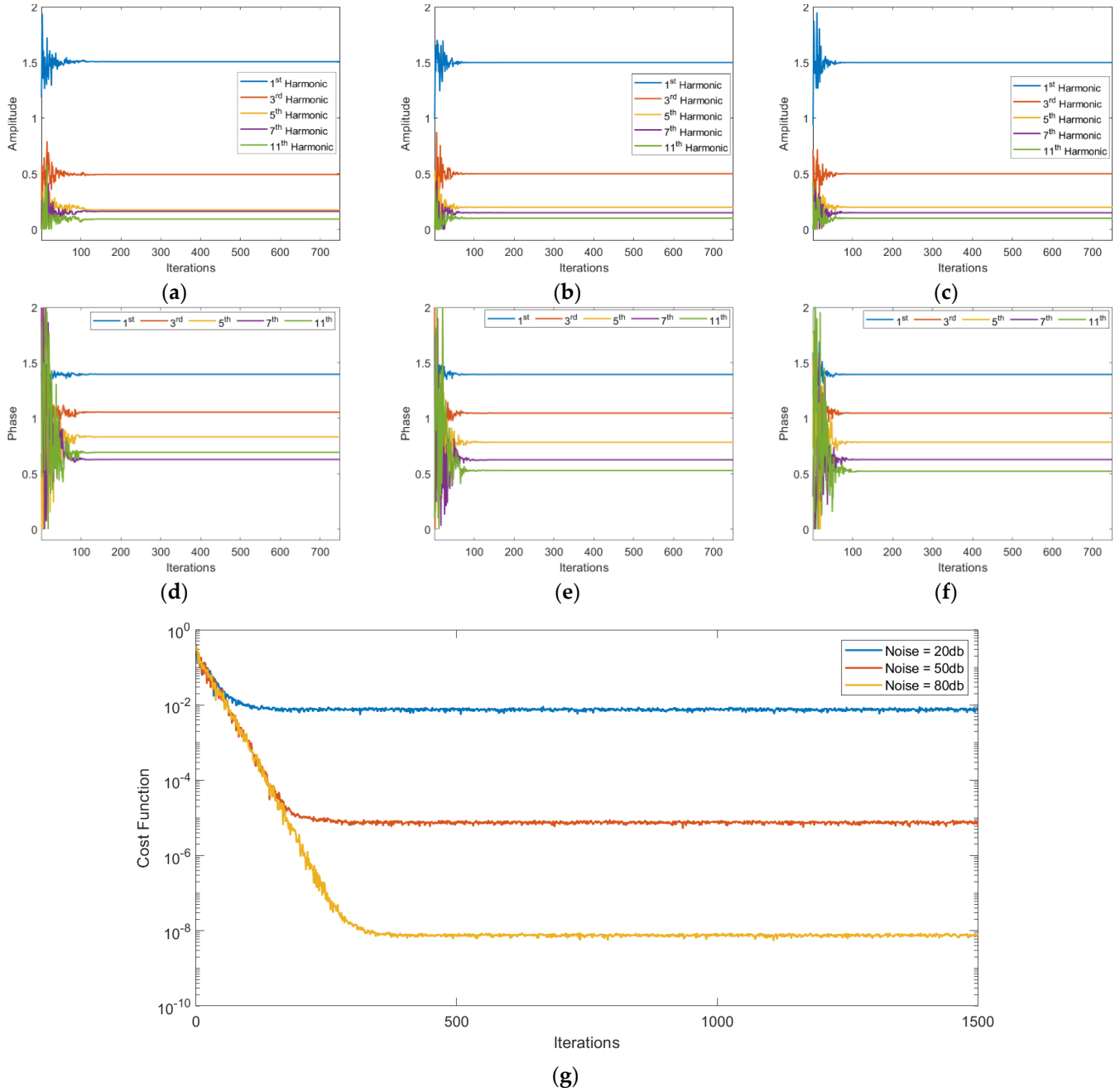

Figure 9. Convergence curves of the harmonic signal in case study 2 for gs = 1500. (**a**) amplitude curves for ε = 20 dB; (**b**) amplitude curves for ε = 50 dB; (**c**) amplitude curves for ε = 80 dB; (**d**) phase curves for ε = 20 dB; (**e**) phase curves for ε = 50 dB; (**f**) phase curves for ε = 80 dB; (**g**) learning curves of the cost function.

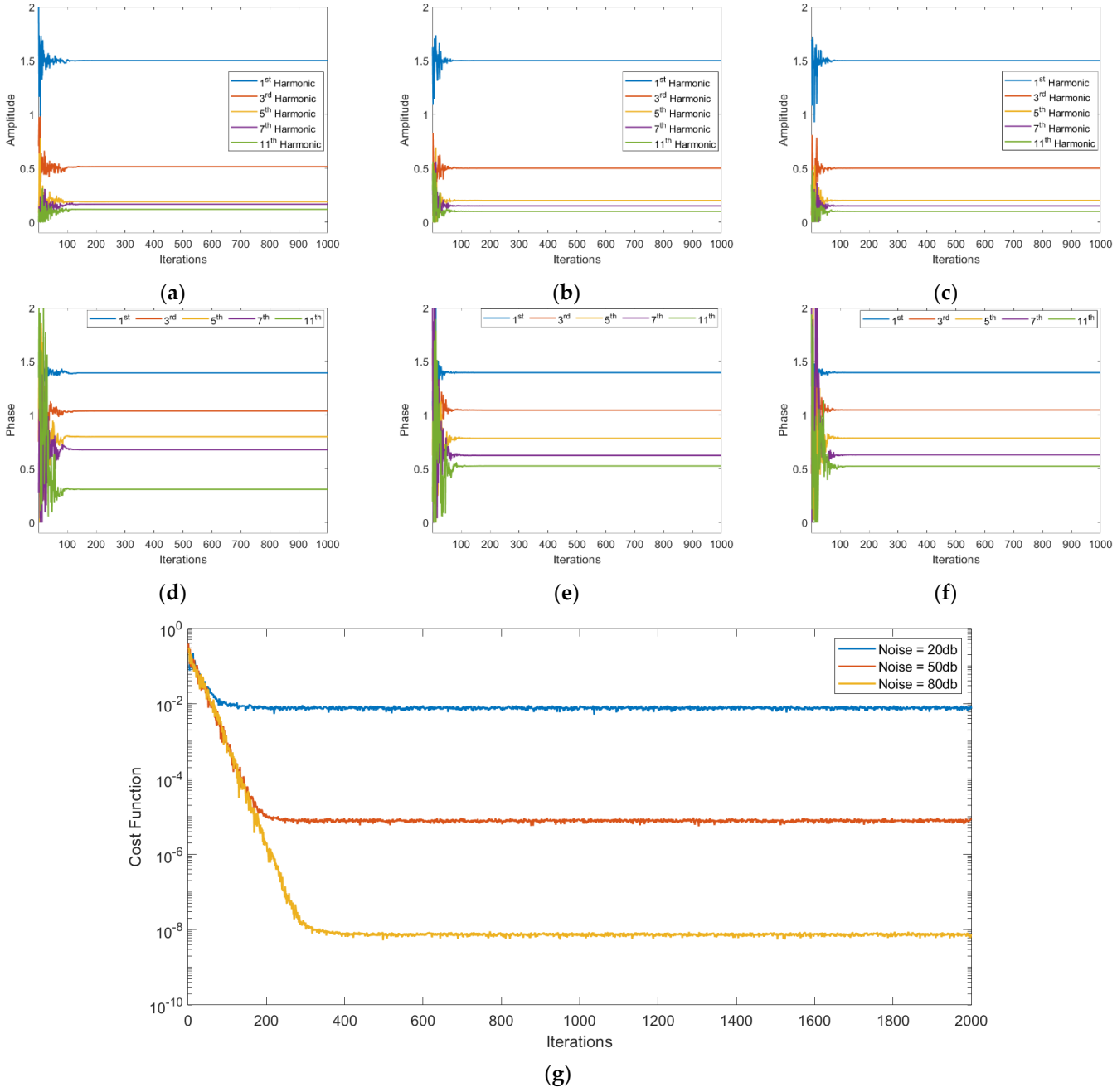

Figure 10. Convergence curves of the harmonic signal in case study 2 for gs = 2000. (**a**) amplitude curves for ε = 20 dB; (**b**) amplitude curves for ε = 50 dB; (**c**) amplitude curves for ε = 80 dB; (**d**) phase curves for ε = 20 dB; (**e**) phase curves for ε = 50 dB; (**f**) phase curves for ε = 80 dB; (**g**) learning curves of the cost function.

5. Conclusions

The swarm intelligence of firefly optimization, FFO, algorithm is exploited for sustainable power systems performance through effectively estimating the harmonics parameters required for mitigating the adverse effects of harmonics on power systems efficiency. The phase and amplitude variables related to the first, third, fifth and eleventh harmonics are successfully estimated through the proposed optimization scheme. The FFO showed robust behavior against different noise conditions, however, increasing the noise level results in relatively decreased value of mean square error based cost function. The accuracy of the FFO scheme enhances for increased particle size, i.e., ps, however, increasing the number

of generations, i.e., gs, has very little impact on accuracy level. The accurate and reliable performance of the FFO makes it an attractive alternative to be exploited in micro grids optimization [59–62]. Moreover, the application of some new algorithms like, Political optimization [63], Harris Hawk optimization [64], Equilibrium optimizer [65], slime mould algorithm [66] and marine predators algorithm [67] to solve parameter estimation problem of power system harmonics looks promising future research direction.

Author Contributions: Conceptualization, N.I.C. and M.A.Z.R.; methodology, N.A.M. and M.A.Z.R.; software, N.A.M.; validation, N.I.C. and M.A.Z.R.; resources, M.A.Z.R.; writing—original draft preparation, N.A.M.; writing—review and editing, N.I.C. and M.A.Z.R. All authors have read and agreed to the published version of the manuscript.

Funding: This research received no external funding.

Institutional Review Board Statement: Not applicable.

Informed Consent Statement: Not applicable.

Data Availability Statement: This manuscript contains no associated data.

Conflicts of Interest: The authors declare no conflict of interest.

References

1. Henderson, R.; Rose, P. Harmonics: The effects on power quality and transformers. *IEEE Trans. Ind. Appl.* **1994**, *30*, 528–532. [CrossRef]
2. Wakileh, G.J. *Power Systems Harmonics: Fundamentals, Analysis and Filter Design*; Springer: Berlin/Heidelberg, Germany, 2019.
3. Rana, R.A.; Patel, S.A.; Muthusamy, A.; Lee, C.W.; Kim, H.-J. Review of Multilevel Voltage Source Inverter Topologies and Analysis of Harmonics Distortions in FC-MLI. *Electronics* **2019**, *8*, 1329. [CrossRef]
4. Biswas, P.P.; Suganthan, P.; Amaratunga, G.A. Minimizing harmonic distortion in power system with optimal design of hybrid active power filter using differential evolution. *Appl. Soft Comput.* **2017**, *61*, 486–496. [CrossRef]
5. Khan, A.; Memon, S.; Sattar, T.P. Analyzing Integrated Renewable Energy and Smart-Grid Systems to Improve Voltage Quality and Harmonic Distortion Losses at Electric-Vehicle Charging Stations. *IEEE Access* **2018**, *6*, 26404–26415. [CrossRef]
6. Martinek, R.; Rzidky, J.; Jaros, R.; Bilik, P.; Ladrova, M. Least Mean Squares and Recursive Least Squares Algorithms for Total Harmonic Distortion Reduction Using Shunt Active Power Filter Control. *Energies* **2019**, *12*, 1545. [CrossRef]
7. Chaudhary, N.I.; Zubair, S.; Raja, M.A.Z. A new computing approach for power signal modeling using fractional adaptive algorithms. *ISA Trans.* **2017**, *68*, 189–202. [CrossRef]
8. Zubair, S.; Chaudhary, N.I.; Khan, Z.A.; Wang, W. Momentum fractional LMS for power signal parameter estimation. *Signal Process.* **2018**, *142*, 441–449. [CrossRef]
9. Chaudhary, N.I.; Latif, R.; Raja, M.A.Z.; Machado, J.T. An innovative fractional order LMS algorithm for power signal parameter estimation. *Appl. Math. Model.* **2020**, *83*, 703–718. [CrossRef]
10. Jain, S.K.; Singh, S. Harmonics estimation in emerging power system: Key issues and challenges. *Electr. Power Syst. Res.* **2011**, *81*, 1754–1766. [CrossRef]
11. Jain, P.; Tiwari, A.K.; Jain, S.K. Harmonic source identification in distribution system using estimation of signal parameters via rotational invariance technique-total harmonic power method. *Trans. Inst. Meas. Control.* **2018**, *40*, 3415–3423. [CrossRef]
12. Lam, H.S.; Li, P.; Chen, B.; Ng, W.M.; Parisini, T.; Hui, S.Y.R. Exponential modulation integral observer for online detection of the fundamental and harmonics in grid-connected power electronics equipment. *IEEE Trans. Control. Syst. Technol.* **2021**, *30*, 1821–1833. [CrossRef]
13. Palczynska, B.; Masnicki, R.; Mindykowski, J. Compressive sensing approach to harmonics detection in the ship electrical network. *Sensors* **2020**, *20*, 2744.
14. D'Antona, G.; Muscas, C.; Sulis, S. State Estimation for the Localization of Harmonic Sources in Electric Distribution Systems. *IEEE Trans. Instrum. Meas.* **2009**, *58*, 1462–1470. [CrossRef]
15. Santos, E.; Khosravy, M.; Lima, M.A.; Cerqueira, A.S.; Duque, C.A. ESPRIT associated with filter bank for power-line harmonics, sub-harmonics and inter-harmonics parameters estimation. *Int. J. Electr. Power Energy Syst.* **2019**, *118*, 105731. [CrossRef]
16. Haider, R.; Kim, C.H.; Ghanbari, T.; Bukhari, S.B.A. Harmonic-signature-based islanding detection in grid-connected distributed generation systems using Kalman filter. *IET Renew. Power Gener.* **2018**, *12*, 1813–1822. [CrossRef]
17. Nie, X. Detection of Grid Voltage Fundamental and Harmonic Components Using Kalman Filter Based on Dynamic Tracking Model. *IEEE Trans. Ind. Electron.* **2019**, *67*, 1191–1200. [CrossRef]
18. Ray, P.K.; Puhan, P.S.; Panda, G. Real time harmonics estimation of distorted power system signal. *Int. J. Electr. Power Energy Syst.* **2016**, *75*, 91–98. [CrossRef]
19. Singh, S.K.; Sinha, N.; Goswami, A.K.; Sinha, N. Variable Constraint based Least Mean Square algorithm for power system harmonic parameter estimation. *Int. J. Electr. Power Energy Syst.* **2015**, *73*, 218–228. [CrossRef]

20. Bhoi, A.; Mallick, R.K.; Panda, G.; Nayak, P. Accurate estimation of modern power system harmonics using a novel LSA hybridized recursive least square technique. *Int. J. Emerg. Electr. Power Syst.* **2021**, *23*, 767–778. [CrossRef]
21. Altaf, F.; Chang, C.-L.; Chaudhary, N.I.; Cheema, K.M.; Raja, M.A.Z.; Shu, C.-M.; Milyani, A.H. Novel Fractional Swarming with Key Term Separation for Input Nonlinear Control Autoregressive Systems. *Fractal Fract.* **2022**, *6*, 348. [CrossRef]
22. Altaf, F.; Chang, C.-L.; Chaudhary, N.I.; Raja, M.A.Z.; Cheema, K.M.; Shu, C.-M.; Milyani, A.H. Adaptive Evolutionary Computation for Nonlinear Hammerstein Control Autoregressive Systems with Key Term Separation Principle. *Mathematics* **2022**, *10*, 1001. [CrossRef]
23. Firouzi, B.; Abbasi, A.; Sendur, P.; Zamanian, M.; Chen, H. Enhancing the performance of Piezoelectric Energy Harvester under electrostatic actuation using a robust metaheuristic algorithm. *Eng. Appl. Artif. Intell.* **2023**, *118*, 105619. [CrossRef]
24. Fé, J.; Correia, S.D.; Tomic, S.; Beko, M. Swarm optimization for energy-based acoustic source localization: A comprehensive study. *Sensors* **2022**, *22*, 1894. [CrossRef] [PubMed]
25. Li, G.; Li, Y.; Chen, H.; Deng, W. Fractional-Order Controller for Course-Keeping of Underactuated Surface Vessels Based on Frequency Domain Specification and Improved Particle Swarm Optimization Algorithm. *Appl. Sci.* **2022**, *12*, 3139. [CrossRef]
26. Mehmood, A.; Chaudhary, N.I.; Zameer, A.; Raja, M.A.Z. Novel computing paradigms for parameter estimation in power signal models. *Neural Comput. Appl.* **2019**, *32*, 6253–6282. [CrossRef]
27. Mehmood, A.; Shi, P.; Raja, M.A.Z.; Zameer, A.; Chaudhary, N.I. Design of backtracking search heuristics for parameter estimation of power signals. *Neural Comput. Appl.* **2020**, *33*, 1479–1496. [CrossRef]
28. Khan, B.S.; Raja, M.A.Z.; Qamar, A.; Chaudhary, N.I. Design of moth flame optimization heuristics for integrated power plant system containing stochastic wind. *Appl. Soft Comput.* **2021**, *104*, 107193. [CrossRef]
29. Muhammad, Y.; Raja, M.A.Z.; Altaf, M.; Ullah, F.; Chaudhary, N.I.; Shu, C.-M. Design of fractional comprehensive learning PSO strategy for optimal power flow problems. *Appl. Soft Comput.* **2022**, *130*, 109638. [CrossRef]
30. Muhammad, Y.; Khan, N.; Awan, S.E.; Raja, M.A.Z.; Chaudhary, N.I.; Kiani, A.K.; Ullah, F.; Shu, C.-M. Fractional memetic computing paradigm for reactive power management involving wind-load chaos and uncertainties. *Chaos Solitons Fractals* **2022**, *161*, 112285. [CrossRef]
31. Ray, P.K.; Subudhi, B. Neuro-evolutionary approaches to power system harmonics estimation. *Int. J. Electr. Power Energy Syst.* **2015**, *64*, 212–220. [CrossRef]
32. Vedik, B.; Shiva, C.K.; Harish, P. Reverse harmonic load flow analysis using an evolutionary technique. *SN Appl. Sci.* **2020**, *2*, 1–11. [CrossRef]
33. Saxena, A.; Kumar, R.; Mirjalili, S. A harmonic estimator design with evolutionary operators equipped grey wolf optimizer. *Expert Syst. Appl.* **2020**, *145*, 113125. [CrossRef]
34. Yao, J.; Yu, H.; Dietz, M.; Xiao, R.; Chen, S.; Wang, T.; Niu, Q. Acceleration harmonic estimation for a hydraulic shaking table by using particle swarm optimization. *Trans. Inst. Meas. Control.* **2016**, *39*, 738–747. [CrossRef]
35. Fernandes, R.A.S.; Oleskovicz, M.; da Silva, I.N. Harmonic source location and identification in radial distribution feeders: An approach based on particle swarm optimization algorithm. *IEEE Trans. Ind. Inform.* **2021**, *18*, 3171–3179. [CrossRef]
36. Hagh, M.T.; Taghizadeh, H.; Razi, K. Harmonic Minimization in Multilevel Inverters Using Modified Species-Based Particle Swarm Optimization. *IEEE Trans. Power Electron.* **2009**, *24*, 2259–2267. [CrossRef]
37. Biswas, S.; Chatterjee, A.; Goswami, S.K. An artificial bee colony-least square algorithm for solving harmonic estimation problems. *Appl. Soft Comput.* **2013**, *13*, 2343–2355. [CrossRef]
38. Kabalci, Y.; Kockanat, S.; Kabalci, E. A modified ABC algorithm approach for power system harmonic estimation problems. *Electr. Power Syst. Res.* **2018**, *154*, 160–173. [CrossRef]
39. Kockanat, S. Acceleration harmonics estimation and elimination with MABC–RLS algorithm: Simulation and experimental analyses on shaking table. *Appl. Soft Comput.* **2020**, *92*, 106377. [CrossRef]
40. Singh, S.K.; Sinha, N.; Goswami, A.K.; Sinha, N. Power system harmonic estimation using biogeography hybridized recursive least square algorithm. *Int. J. Electr. Power Energy Syst.* **2016**, *83*, 219–228. [CrossRef]
41. Malik, N.A.; Chang, C.-L.; Chaudhary, N.I.; Raja, M.A.Z.; Cheema, K.M.; Shu, C.-M.; Alshamrani, S.S. Knacks of Fractional Order Swarming Intelligence for Parameter Estimation of Harmonics in Electrical Systems. *Mathematics* **2022**, *10*, 1570. [CrossRef]
42. Malik, N.A.; Chang, C.-L.; Chaudhary, N.I.; Khan, Z.A.; Raja, M.A.Z.; Kiani, A.K.; Milyani, A.H.; Azhari, A.A. Parameter estimation of harmonics arising in electrical instruments of smart grids using cuckoo search heuristics. *Front. Energy Res.* **2022**, *10*, 1733. [CrossRef]
43. Yang, X.S.; Slowik, A. Firefly algorithm. In *Swarm Intelligence Algorithms*; CRC Press: Boca Raton, FL, USA, 2020; pp. 163–174.
44. Kumar, V.; Kumar, D. A systematic review on firefly algorithm: Past. 2021, present, and future. *Arch. Comput. Methods Eng.* **2020**, *28*, 3269–3291. [CrossRef]
45. Yin, P.-Y.; Chen, P.-Y.; Wei, Y.-C.; Day, R.-F. Cyber Firefly Algorithm Based on Adaptive Memory Programming for Global Optimization. *Appl. Sci.* **2020**, *10*, 8961. [CrossRef]
46. Abo-Khalil, A.G.; Alharbi, W.; Al-Qawasmi, A.R.; Alobaid, M.; Alarifi, I.M. Maximum power point tracking of PV systems under partial shading conditions based on opposition-based learning firefly algorithm. *Sustainability* **2021**, *13*, 2656. [CrossRef]
47. Watanabe, R.B.; Junior, O.H.A.; Leandro, P.G.M.; Salvadori, F.; Beck, M.F.; Pereira, K.; Brandt, M.H.M.; de Oliveira, F.M. Implementation of the Bio-Inspired Metaheuristic Firefly Algorithm (FA) Applied to Maximum Power Point Tracking of Photovoltaic Systems. *Energies* **2022**, *15*, 5338. [CrossRef]

48. Nazeri, M.; Tajuddin, M.; Babu, T.; Azmi, A.; Malvoni, M.; Kumar, N. Firefly Algorithm-Based Photovoltaic Array Reconfiguration for Maximum Power Extraction during Mismatch Conditions. *Sustainability* **2021**, *13*, 3206. [CrossRef]
49. Yousif, A.; Alqhtani, S.M.; Bashir, M.B.; Ali, A.; Hamza, R.; Hassan, A.; Tawfeeg, T.M. Greedy firefly algorithm for optimizing job scheduling in iot grid computing. *Sensors* **2022**, *22*, 850. [CrossRef]
50. Jovanovic, D.; Antonijevic, M.; Stankovic, M.; Zivkovic, M.; Tanaskovic, M.; Bacanin, N. Tuning Machine Learning Models Using a Group Search Firefly Algorithm for Credit Card Fraud Detection. *Mathematics* **2022**, *10*, 2272. [CrossRef]
51. Huang, J.; Sabri, M.M.S.; Ulrikh, D.V.; Ahmad, M.; Alsaffar, K.A.M. Predicting the compressive strength of the cement-fly ash–slag ternary concrete using the firefly algorithm (fa) and random forest (rf) hybrid machine-learning method. *Materials* **2022**, *15*, 4193. [CrossRef]
52. Fajuke, I.D.; Raji, A.K. Firefly Algorithm-Based Optimization of the Additional Energy Yield of Bifacial PV Modules. *Energies* **2022**, *15*, 2651. [CrossRef]
53. Kaur, M.; Prashar, D.; Rashid, M.; Khanam, Z.; Alshamrani, S.S.; AlGhamdi, A.S. An Optimized Load Balancing Using Firefly Algorithm in Flying Ad-Hoc Network. *Electronics* **2022**, *11*, 252. [CrossRef]
54. Behera, M.; Sarangi, A.; Mishra, D.; Mallick, P.K.; Shafi, J.; Srinivasu, P.N.; Ijaz, M.F. Automatic Data Clustering by Hybrid Enhanced Firefly and Particle Swarm Optimization Algorithms. *Mathematics* **2022**, *10*, 3532. [CrossRef]
55. Ikotun, A.M.; Ezugwu, A.E. Enhanced Firefly-K-Means Clustering with Adaptive Mutation and Central Limit Theorem for Automatic Clustering of High-Dimensional Datasets. *Appl. Sci.* **2022**, *12*, 12275. [CrossRef]
56. Huang, L.; Jiang, L.; Zhao, L.; Ding, X. Temperature compensation method based on an improved firefly algorithm optimized backpropagation neural network for micromachined silicon resonant accelerometers. *Micromachines* **2022**, *13*, 1054. [CrossRef] [PubMed]
57. Zedadra, O.; Guerrieri, A.; Seridi, H. LFA: A Lévy Walk and Firefly-Based Search Algorithm: Application to Multi-Target Search and Multi-Robot Foraging. *Big Data Cogn. Comput.* **2022**, *6*, 22. [CrossRef]
58. Li, Y.; Li, J.; Sun, Y.; Li, H. Load Balancing Based on Firefly and Ant Colony Optimization Algorithms for Parallel Computing. *Biomimetics* **2022**, *7*, 168. [CrossRef]
59. Ju, Y.; Liu, W.; Wang, J.; Li, J.; Huang, Y.; Chen, X.; Dong, Z. Power flow analysis of integrated energy microgrid considering non-smooth characteristics. IET Generation. *Transm. Distrib.* **2020**, *16*, 2777–2790. [CrossRef]
60. Ju, Y.; Liu, W.; Zhang, Z.; Zhang, R. Distributed Three-Phase Power Flow for AC/DC Hybrid Networked Microgrids Considering Converter Limiting Constraints. *IEEE Trans. Smart Grid.* **2022**, *13*, 1691–1708. [CrossRef]
61. Huang, Y.; Ju, Y.; Ma, K.; Short, M.; Chen, T.; Zhang, R.; Lin, Y. Three-phase optimal power flow for networked microgrids based on semidefinite programming convex relaxation. *Appl. Energy* **2022**, *305*, 117771. [CrossRef]
62. Ju, Y.; Wang, J.; Zhang, Z.; Huang, Y.; Lin, Y. A Calculation Method for Three-Phase Power Flow in Micro-Grid Based on Smooth Function. *IEEE Trans. Power Syst.* **2020**, *35*, 4896–4903. [CrossRef]
63. Askari, Q.; Younas, I.; Saeed, M. Political Optimizer: A novel socio-inspired meta-heuristic for global optimization. *Knowl. Based Syst.* **2020**, *195*, 105709. [CrossRef]
64. Heidari, A.A.; Mirjalili, S.; Faris, H.; Aljarah, I.; Mafarja, M.; Chen, H. Harris hawks optimization: Algorithm and applications. *Future Gener. Comput. Syst.* **2019**, *97*, 849–872. [CrossRef]
65. Faramarzi, A.; Heidarinejad, M.; Stephens, B.; Mirjalili, S. Equilibrium optimizer: A novel optimization algorithm. *Knowl. Based Syst.* **2019**, *191*, 105190. [CrossRef]
66. Li, S.; Chen, H.; Wang, M.; Heidari, A.A.; Mirjalili, S. Slime mould algorithm: A new method for stochastic optimization. *Future Gener. Comput. Syst.* **2020**, *111*, 300–323. [CrossRef]
67. Faramarzi, A.; Heidarinejad, M.; Mirjalili, S.; Gandomi, A.H. Marine Predators Algorithm: A nature-inspired metaheuristic. *Expert Syst. Appl.* **2020**, *152*, 113377. [CrossRef]

Disclaimer/Publisher's Note: The statements, opinions and data contained in all publications are solely those of the individual author(s) and contributor(s) and not of MDPI and/or the editor(s). MDPI and/or the editor(s) disclaim responsibility for any injury to people or property resulting from any ideas, methods, instructions or products referred to in the content.